Acta Crystallographica Section D
Biological Crystallography
ISSN 0907-4449

Unusual non-crystallographic symmetry in crystals of a 420 kDa crustacean clottable protein

Justin M. Kollman and Russell F. Doolittle*

Center for Molecular Genetics, University of California, San Diego, La Jolla, CA 92093-0634, USA

Correspondence e-mail: rdoolittle@ucsd.edu

Received 6 November 2004
Accepted 11 January 2005

The 420 kDa hemolymph clottable protein has been purified from the California spiny lobster *Panulirus interrruptus* and crystallized in both monoclinic and orthorhombic space groups. Complete data sets have been collected from the two crystal forms to a maximum resolution of 3.9 and 3.2 Å, respectively. The monoclinic crystals exhibit unusual noncrystallographic symmetry with pseudo-ninefold rotational symmetry generated from three dimers per asymmetric unit. The orthorhombic crystals have a single dimer per asymmetric unit. Attempts to phase the data are currently under way.

1. Introduction

The various animal phyla have evolved distinct clotting systems that prevent the loss of circulatory fluids. In crustaceans, the clot is formed by the polymerization of a 420 kDa homodimeric circulating clottable protein (CP) by the action of a calcium-dependent transglutaminase that introduces covalent bonds between CP dimers. The amino-acid sequence of CP showed it to be related to vitellogenins (lipovitellins), which are lipid-binding transport proteins found in egg-laying animals; indeed, 5% of the weight of CP is bound astaxanthin, a hydrophobic carotenoid pigment (Doolittle & Riley, 1990; Hall *et al.*, 1999; Fuller & Doolittle, 1971*a*,*b*).

The common ancestry of lipovitellin and CP reflects a rather straightforward evolutionary history. Either the gene for vitellogenin was duplicated to create the new clotting protein or the vitellogenin itself acquired new features. In either case, the protein became a suitable substrate for cross-linking by a transglutaminase, a class of enzymes found in most animal tissues. Comparison of the three-dimensional structure of CP with that of lipovitellin (Anderson *et al.*, 1998) should illuminate the details of these evolutionary changes.

We have purified CP from the California spiny lobster *Panulirus interruptus* and crystallized it in two different forms. The orthorhombic form has a single dimer in the asymmetric unit, whereas the monoclinic form has an unusual pseudo-ninefold rotational symmetry generated from three CP dimers in the asymmetric unit.

2. Purification

Crude CP was purified essentially as described in Fuller & Doolittle (1971*a*). Lobster hemolymph was collected into an anticoagulant solution consisting of 100 m*M* sodium citrate/50 m*M* EDTA at 277 K and hemocytes were removed by centrifugation. The hemolymph supernatant was dialyzed overnight against four changes of 50 m*M* Tris/10 m*M* EDTA pH 8.0 at a buffer-to-hemolymph ratio of about 20:1. The pH of the hemolymph supernatant was lowered to 5.0 by the dropwise addition of 0.1 *M* sodium acetate pH 4.0. CP precipitated at this pH and was pelleted by centrifugation. The pellet was dissolved in 100 m*M* Tris/10 m*M* EDTA pH 8.0, dialyzed against 50 m*M* Tris/10 m*M* EDTA pH 8.0 and re-precipitated as above. The final pellet was dissolved in 50 m*M* glycine/1 m*M* EDTA pH 10.1 and dialyzed against the same buffer. The high pH serves to dissociate the subunits of hemocyanin, a major contaminant.

The crude CP solution was applied onto a 2.5 × 165 cm Sepharose CL-6B column. Two major peaks eluted from the column corresponding to CP and cross-linked CP. The incomplete resolution of the two peaks required the CP pool to be further purified by a second

passage over the same column. Purified CP was dialyzed against 2.5 m*M* Tris, 1 m*M* EDTA pH 7.8, concentrated to 10–20 mg ml^{-1} and stored at 203 K. The bright orange color of the final preparation indicates that astaxanthin remained bound to the protein throughout purification. The final yield of purified CP was roughly 0.15 mg per millilitre of decalcified hemolymph.

For some crystallization experiments, CP was deglycosylated. Purified CP was diluted to 1 mg ml^{-1} in 50 m*M* sodium acetate/300 m*M* sodium chloride pH 5.0 and 2.5 µU endoglycosidase F2 (CalBiochem) was added. The reaction was allowed to proceed for 24 h at 277 K. The protein was then dialyzed extensively against 2.5 m*M* Tris, 1 m*M* EDTA pH 7.8 and concentrated to 10–20 mg ml^{-1}.

3. Crystallization

All crystals were grown by vapor diffusion in sitting-drop plates with 1 ml well solution. Variously sized drops were set up as 1:1 mixtures of the well solution and concentrated protein solution. Initial limited screens were carried out on protein purified in 1977 that had been stored at 203 K. Remarkably, small crystals of this decades-old protein developed within a week using PEG 3350 as the precipitant. Fresh protein was purified and crystallization conditions were optimized to give larger crystals from a well solution of 5%(*w*/*v*) PEG 3350, 10 m*M* $MnCl_2$ and 0.1 *M* PIPES pH 7.2 and 10 mg ml^{-1} protein solution. A microcrystalline precipitate formed in these drops within several days and diffraction-quality crystals grew within 1–2 weeks (Fig. 1*a*). Both the size and diffraction quality of these crystals were enhanced by deglycosylation of the protein. Occasionally, crystals could be grown with a longest dimension of 1 mm, although they more typically reached 0.2–0.4 mm. Crystals were cryoprotected by 1 min sequential soaks in well solutions containing 5, 10 and 15%(*v*/*v*) 2-methyl 2,4-pentanediol (MPD) and were then frozen and stored in liquid nitrogen.

Table 1
Data-collection statistics.

Values in parentheses are for the highest resolution shell.

Space group	$P2_1$	$P2_12_12_1$
Unit-cell parameters (Å, °)	a = 149.6, b = 158.4, c = 325.1, β = 93.4	a = 121.8, b = 183.6, c = 187.4
Resolution (Å)	50–3.9	50–3.2
Completeness (%)	95.2 (90.2)	99.9 (100)
$R_{\rm merge}$†	0.096 (0.497)	0.083 (0.446)
$\langle I/\sigma(I)\rangle$	10.25 (2.56)	14.07 (4.97)
Total reflections	464508	432857
Unique reflections	151188	68685
Mosaicity (°)	0.67	0.35
Dimers per AU	3	1
Solvent content‡ (%)	58.6	52.7

† $R_{\rm merge} = \sum_{hkl}\sum_i |I_i(hkl) - \langle I(hkl)\rangle| / \sum_{hkl}\sum_i (hkl)$. ‡ The solvent content was calculated based on the measured crystal density of the monoclinic crystals. For the orthorhombic crystals, one CP dimer was assumed per asymmetric unit.

The density of these monoclinic crystals was determined in Ficoll gradients by the method of Westbrook (1985), with mixtures of benzene and toluene as density standards. The average of four independent density measurements was 1.168 g cm^{-3}, with a standard

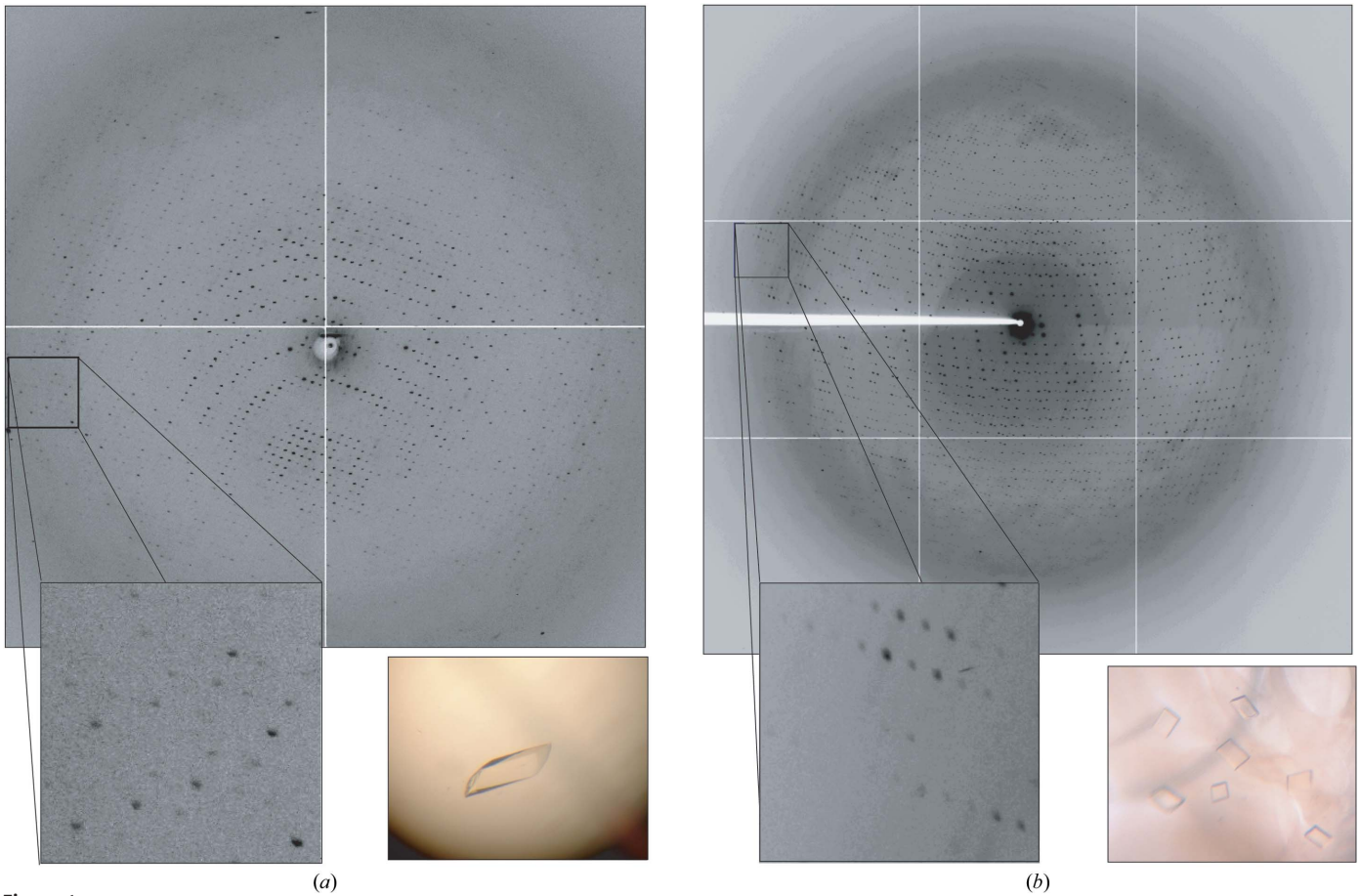

(*a*) (*b*)

Figure 1
Two forms of lobster CP crystals and their diffraction patterns. (*a*) Monoclinic, (*b*) orthorhombic.

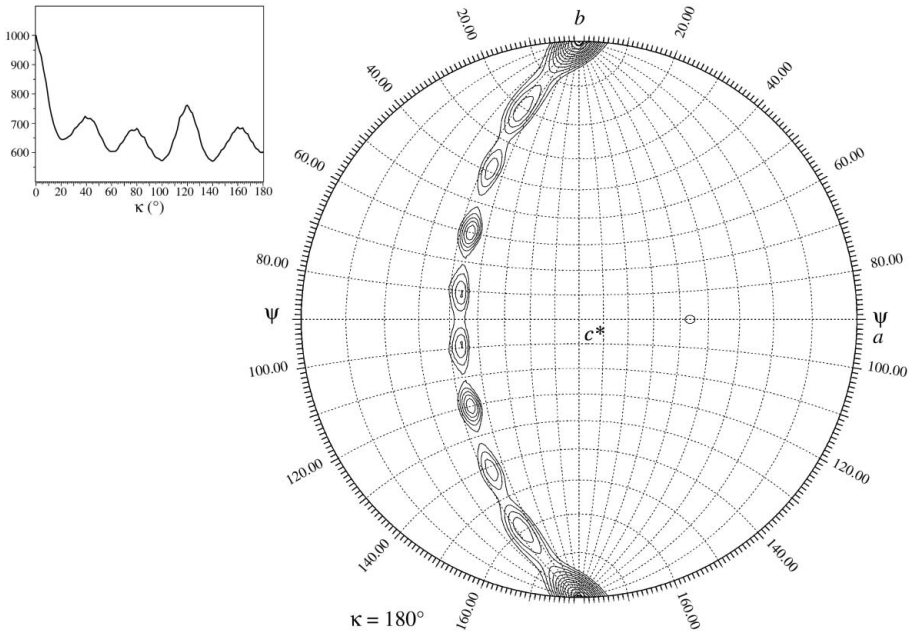

Figure 2
Self-rotation function of monoclinic CP crystals. An apparent ninefold axis lies along $\varphi = 46$, $\psi = 90°$, generating peaks on $\kappa = 40$, 80, 120 and 160° (inset). Perpendicular to the pseudo-ninefold axis are nine peaks on $\kappa = 180°$. Data in the resolution range 10–4.5 Å were used, with a total of 69 302 reflections and 8527 large terms and a search radius of 30 Å. The map is contoured from 4σ to 7σ at 0.25σ intervals.

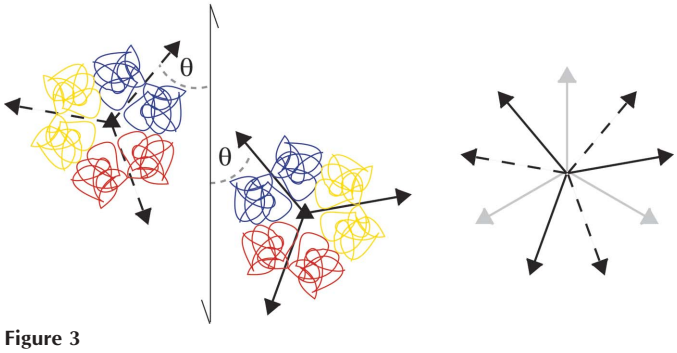

Figure 3
Model of noncrystallographic symmetry in monoclinc crystals. The asymmetric unit consists of an assembly of three CP dimers with their dimeric twofold axes perpendicular to a threefold rotational axis. This assembly is arranged such that one of the twofold axes forms an angle θ of 40° with the crystallographic screw axis (left). Superposition of the symmetry elements (right) generates a third set of twofold relationships (gray arrows), which results in pseudo-ninefold symmetry.

deviation of 0.004 g cm^{-3}. Application of the Matthews equation for the protein content of crystals (Matthews, 1968) showed the number of CP dimers per asymmetric unit to be 3.2.

A second crystal form was discovered in a broader screen. The optimal conditions for growth of these crystals were a well solution consisting of 8%(*v*/*v*) MPD and 50 m*M* sodium acetate pH 5.2 mixed 1:1 in the drop with 10 mg ml^{-1} protein stock solution. Under these conditions, a cloudy precipitate formed immediately and small crystals grew within 2–5 d (Fig. 1*b*). These crystals were extremely pH-sensitive and small crystals of this type grew even in the absence of MPD, suggesting that isoelectric precipitation is the driving force behind crystal growth in this instance. Interestingly, deglycosylated protein did not form crystals under these conditions. These crystals typically grew as thin plates, with the thinnest dimension rarely exceeding 0.01 mm. These crystals were cryoprotected by the same sequential procedure used for the monoclinic crystals, but with a final MPD concentration of 20%(*v*/*v*).

4. Data collection

Monoclinic crystals were screened for diffraction quality on an in-house X-ray source. Complete data sets were collected at Advanced Light Source beamline 5.0.2 on an ADSC Quantum 210 CCD detector at 100 K. Individual reflections could be detected out to about 3.5 Å (Fig. 1*a*), but anisotropic diffraction limited the useful limit to about 3.9 Å. The crystals belong to space group $P2_1$, with unit-cell parameters $a = 149.6$, $b = 158.4$, $c = 325.1$ Å, $\beta = 93.4°$ (Table 1).

The orthorhombic crystals diffracted poorly on an in-house X-ray source (typically to less than 8 Å), probably owing to their very small size. Therefore, these crystals were screened and data sets collected at Advanced Light Source beamline 8.2.2 on an ADSC Quantum 315 CCD detector at 100 K (Fig. 1*b*). These crystals belong to space group $P2_12_12_1$, with unit-cell parameters $a = 121.8$, $b = 183.6$, $c = 187.4$ Å (Table 1). Individual reflections were observed out to 2.9 Å, but the average $I/\sigma(I)$ drops off very rapidly beyond about 3.2 Å.

Data sets were indexed, integrated and scaled with the *HKL* software package (Otwinowski & Minor, 1997). A summary of the processed data is presented in Table 1.

5. Noncrystallographic symmetry

Self-rotation functions were calculated for both crystal forms using the program *GLRF* (Tong & Rossmann, 1997). The orthorhombic crystals display a single peak in the self-rotation function, on the $\kappa = 180°$ plane, presumably representing a twofold rotational axis relating the two disulfide-linked halves of the CP dimer. However, the monoclinic crystals exhibit an unusual self-rotation function (Fig. 2). In this case, there are clearly nine peaks on the $\kappa = 180°$ plane, spaced at 20° intervals along $\varphi = 135°$. Peaks occur normal to the twofold peaks along $\varphi = 45$, $\psi = 90°$ at 40° intervals along κ. This strongly suggests ninefold rotational symmetry. However, the calculated solvent content for these crystals with nine CP dimers in the asymmetric unit is less than zero and it is difficult to conceive of a situation in which 4.5 dimers could be arranged in each asymmetric unit to give ninefold symmetry.

Measurement of the crystal density indicated that there were only three dimers in the asymmetric unit, suggesting a model which accounts for the apparent ninefold NCS. In this model, three CP dimers are arranged with their dimeric twofold axes perpendicular to a threefold axis. The trimer of dimers is positioned so that one of the dimeric axes forms an angle θ of about 40° with the crystallographic screw axis (Fig. 3*a*). Because CP is a dimer, rotation of this assembly about the screw axis is equivalent to a 40° rotation about the threefold axis. The symmetry elements from the two asymmetric units interact to generate the apparent ninefold symmetry (Fig. 3*b*).

To confirm that this reasoning accounts for the observed NCS, a model was generated using the structure of a CP homolog, lamprey lipovitellin (Anderson *et al.*, 1998), arranged as described and placed in the crystal unit cell. Structure factors were generated for the model using the program *TF* (Tong & Rossmann, 1997). The calculated self

rotation closely resembles the self rotation of the crystal data (Fig. 4*a*). The pseudo-ninefold symmetry is observed with angles θ in the range 40–45° (Fig. 4*b*). Although the diffraction limit of the monoclinic crystal data is only 3.9 Å, NCS averaging over the six CP monomers in the asymmetric unit may eventually provide a high-quality electron-density map.

Even though the model suggests a trimer of CP dimers in the asymmetric unit, it is likely that the trimer is only the result of crystal packing. Neither negative-staining electron microscopy (Fuller & Doolittle, 1971*b*; Hall *et al.*, 1999) nor extensive cryoelectron microscopy (data not shown) indicate that CP adopts a trimeric form in solution or in the clot.

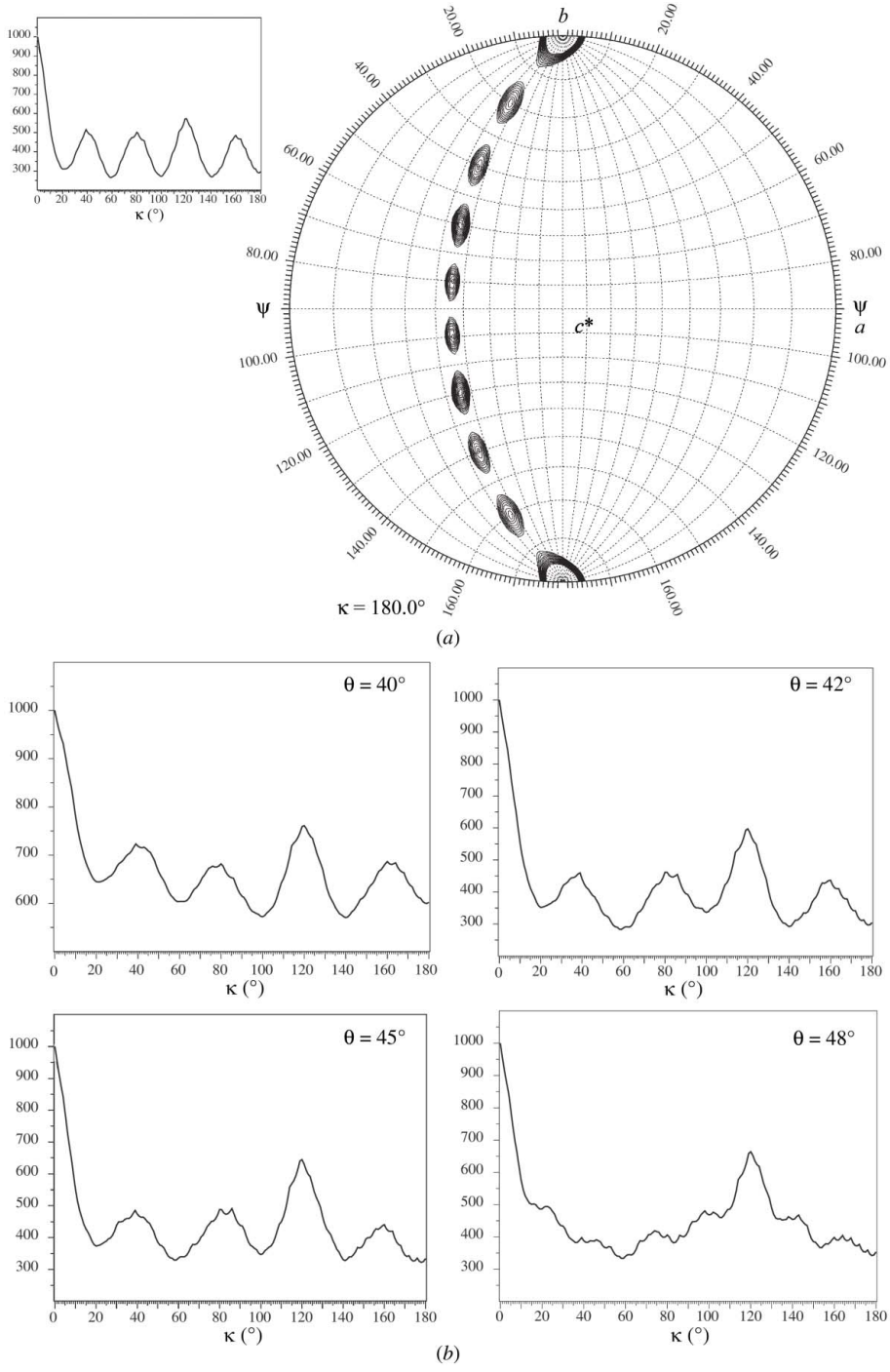

Figure 4
Self-rotation function of noncrystallographic symmetry model. (*a*) The self-rotation function of the model described in Fig. 3, calculated and contoured as in Fig. 2. 11 310 large terms were used from a total of 85 549 reflections. (*b*) The pseudo-ninefold rotational symmetry is dependent on the angle θ between the crystallographic screw axis and the dimeric twofold axes (Fig. 3). At $\theta < 45°$ the ninefold axis is still recognizable, but at greater angles only the peak at $\kappa = 120°$ remains strong.

6. Attempts at phasing

Although the homology between lipovitellin and CP is clear (Doolittle & Riley, 1990; Hall *et al.*, 1999), the overall sequence identity between the two is less than 25%. Nonetheless, attempts were made to solve the CP structure by molecular replacement, with the structure of lamprey lipovitellin (PDB code 1lsh) as a search model. While marginal rotation-search peaks were found using the locked rotation function on the monoclinic crystal data with the program *GLRF* (Tong & Rossmann, 1997), the translation search did not return a solution. Other molecular-replacement programs were used, including *AMoRe* (Navaza, 1994), *EPMR* (Kissinger *et al.*, 1999), *FSEARCH* (Hao, 2001) and *PHASER* (Storoni *et al.*, 2004). The lipovitellin dimer, monomer and separate domains were used as search models to no avail.

Hundreds of heavy-atom soaking conditions have been screened in a search for useful derivatives to solve the structure by multiple isomorphous replacement. These efforts were focused on the orthorhombic crystals because of their smaller unit cell, higher diffraction limit and less complicated noncrystallographic symmetry, although some conditions have also been screened with the monoclinic crystals. None of the conditions tried so far has yielded a useful derivative. The large size of the crystal asymmetric unit as well as the fact that the orthorhombic crystals must be screened on a synchrotron X-ray source have contributed to the difficulties in finding useful derivatives.

Experiments are currently under way to determine a low-resolution structure by single-particle reconstruction from electron micrographs of individual CP molecules embedded in vitreous ice. This structure may prove useful in obtaining initial phases for the diffraction data.

We would like to thank Ed Kisfaludy of the Scripps Institute of Oceanography for capturing lobsters, Professor Partho Ghosh for help with crystallization screening, Michael Sawaya for helpful discussions about NCS and the staff at the Advanced

Light Source for assistance with data collection.

References

Anderson, T. A., Levitt, D. G. & Banaszak, L. J. (1998). *Structure*, **15**, 895–909.
Doolittle, R. F. & Riley, M. (1990). *Biochem. Biophys. Res. Commun.* **167**, 16–19.
Fuller, G. M. & Doolittle, R. F. (1971*a*). *Biochemistry*, **10**, 1305–1311.
Fuller, G. M. & Doolittle, R. F. (1971*b*). *Biochemistry*, **10**, 1311–1315.
Hall, M., Wang, R., van Antwerpen, R., Sottrup-Jensen, L. & Soderhall, K. (1999). *Proc. Natl Acad. Sci. USA*, **96**, 1965–1970.
Hao, Q. (2001). *Acta Cryst.* D**57**, 1410–1414.
Kissinger, C. R., Gehlhaar, D. K. & Fogel, D. B. (1999). *Acta Cryst.* D**55**, 484–491.
Matthews, B. W. (1968). *J. Mol. Biol.* **33**, 491–497.
Navaza, J. (1994). *Acta Cryst.* A**50**, 157–163.
Otwinowski, Z. & Minor, W. (1997). *Methods Enzymol.* **276**, 307–326.
Storoni, L. C., McCoy, A. J. & Read, R. J. (2004). *Acta Cryst.* D**60**, 432–438.
Tong, L. & Rossmann, M. G. (1997). *Methods Enzymol.* **276**, 594–611.
Westbrook, E. M. (1985). *Methods Enzymol.* **114**, 187–196.